JGR Atmospheres

RESEARCH ARTICLE
10.1029/2020JD034198

Key Points:

- The convective-to-total precipitation (PC/PR) ratio is too high in many Climate Model Intercomparison Project Phase 5 (CMIP5) models in the tropics
- The high PC/PR ratios are associated with the "drizzling" bias
- A few CMIP6 models show reduced PC/PR ratio and "drizzling" bias

Supporting Information:

Supporting Information may be found in the online version of this article.

Correspondence to:

D. Chen,
dichen@atmos.ucla.edu

Citation:

Chen, D., Dai, A., & Hall, A. (2021). The convective-to-total precipitation ratio and the "drizzling" bias in climate models. *Journal of Geophysical Research: Atmospheres*, *126*, e2020JD034198. https://doi.org/10.1029/2020JD034198

Received 4 NOV 2020
Accepted 26 JUL 2021

The Convective-To-Total Precipitation Ratio and the "Drizzling" Bias in Climate Models

Di Chen[1], Aiguo Dai[2], and Alex Hall[1]

[1]Department of Atmospheric and Oceanic Sciences, University of California, Los Angeles, Los Angeles, CA, USA, [2]Department of Atmospheric and Environmental Sciences, University at Albany, State University of New York, Albany, NY, USA

Abstract Overestimation of precipitation frequency and duration while underestimating intensity, that is, the "drizzling" bias, has been a long-standing problem of global climate models. Here we explore this issue from the perspective of precipitation partitioning. We found that most models in the Climate Model Intercomparison Project Phase 5 (CMIP5) have high convective-to-total precipitation (PC/PR) ratios in low latitudes. Convective precipitation has higher frequency and longer duration but lower intensity than non-convective precipitation in many models. As a result, the high PC/PR ratio contributes to the "drizzling" bias over low latitudes. The PC/PR ratio and associated "drizzling" bias increase as model resolution coarsens from 0.5° to 2.0°, but the resolution's effect weakens as the grid spacing increases from 2.0° to 3.0°. Some of the CMIP6 models show reduced "drizzling" bias associated with decreased PC/PR ratio. Thus, more reasonable precipitation partitioning, along with finer model resolution should alleviate the "drizzling" bias within current climate models.

Plain Language Summary Precipitation occurs more frequently and lasts longer but with lower intensity in global climate models than in the real world. We explore this issue from the perspective of precipitation partitioning, that is, how total precipitation is divided into convective and non-convective components in models. We find that most CMIP5 models produce too much convective but too little non-convective precipitation in low latitudes. Convective precipitation is generally more drizzle-like than non-convective precipitation in models. This contributes to the "drizzling" bias at low latitudes. Climate models with coarser resolution typically have higher convective-to-total ratios and larger "drizzling" biases. Hence, more realistic precipitation partitioning and smaller grid spacing should help reduce the "drizzling" bias.

1. Introduction

Global climate models (GCMs) are known to have a "drizzling" bias that is, characterized by unrealistically high precipitation frequency (F) and duration (D) but low intensity (I), even though precipitation amount (A) is realistic (Dai, 2006; DeMott et al., 2007; Zhou et al., 2008). Despite many efforts (e.g., Zhang, 2002; Xie et al., 2004; Zhang & Mu, 2005) to address this long-standing problem, it persists for generations of GCMs (Chen & Dai, 2019; Flato et al., 2013; Stephen et al., 2010; Trenberth & Zhang, 2018). The "drizzling" bias impedes realistic representation of precipitation characteristics, as well as projections of future hydrologic extremes (Trenberth, 2011; Trenberth et al., 2003). It also contributes to biases in model-simulated land surface processes by increasing surface evaporation and decreasing runoff (Qian et al., 2006). The issue is more prominent at sub-daily timescales, at which the majority of extreme events occur (Westra et al., 2014). Although cloud-resolving regional models simulate more realistic precipitation (e.g., Dai et al., 2020; Prein et al., 2017), GCMs remain our primary tool for studying current climate and projecting future climate changes. Therefore, to improve the credibility of GCMs, we need to understand and reduce their "drizzling" bias.

Too frequent and premature occurrence of moist convection is found in models compared with observations (Chen & Dai, 2019; Dai & Trenberth, 2004; DeMott et al., 2007). In reality, atmospheric instability often accumulates because of convective inhibition (CIN) or negative buoyancy before intense convection starts (Chen et al., 2020; Dai, 2006; Dai & Trenberth, 2004). Chen and Dai (2019) found that in recent versions of the Community Atmosphere Model (CAM4 & CAM5), convective precipitation generated by the cumulus

parameterization is too frequent and long-lasting with reduced intensity, and it unrealistically dominates total precipitation, leading to the "drizzling" bias. Model-simulated convective precipitation is affected by several aspects of the convective parameterization. These include the closure, convective trigger, entrainment rate, the spectrum of the convective and mesoscale clouds, and other parameters whose physical basis is not well understood (Wilcox & Donner, 2007). DeMott et al. (2007) suggests that the small entrainment rate in the Zhang and McFarlane (1995; hereafter ZM95) convective parameterization inhibits shallow convection, thereby impeding the moistening of the environment and subsequent development of deep and intense convection in CAM. Suppression mechanisms based on relative humidity thresholds or a precondition of positive low-level moisture convergence lead to overall smaller biases (Rosa & Collins, 2013). In addition, decreasing the convective available potential energy (CAPE) consumption time scale or increasing model time step can increase the strength of convection in CAM (Williamson, 2013).

Meanwhile, precipitation partitioning can also be altered by the use of different cloud microphysics schemes, which produce the resolved non-convective (or large-scale) precipitation in models. Even with the same ZM95 convective parameterization, convective and non-convective precipitation characteristics vary considerably when different cloud microphysics schemes are used in current and previous versions of CAM (Chen & Dai, 2019; Gettelman et al., 2008). Interactions of cumulus and microphysics schemes also modulate the convective and large-scale precipitation amount (Held et al., 2007; Lin et al., 2013). Previous studies (e.g., Lin et al., 2013; Rauscher et al., 2016) found that the simulated non-convective precipitation is closely coupled to the low-level convergence and surface heat flux. Meanwhile, large-scale processes (e.g., lower tropospheric moisture divergence) interact with convective schemes and influence the spatiotemporal distributions of convective precipitation (Sakaguchi et al., 2018). In addition, cumulus and microphysics parameterizations jointly determine low-latitudes cloud cover (Ma et al., 2018), which impacts Earth's radiation budget and precipitation. To produce more realistic total precipitation, it is recommended to give more credit to large-scale processes in models (Kooperman et al., 2018).

The coarse spatial resolution of many GCMs is found to be partly responsible for the "drizzling" bias (Stephens et al., 2010). The influence of model resolution is two-fold (Chen & Dai, 2019). The first impact is from the area aggregation effect–as the spatial sampling area or the size of grid box increases, the probability or frequency of precipitation increases (Chen & Dai, 2018). The second effect comes from increased contribution from parameterized convective precipitation as model resolution decreases. In CAM, finer resolution improves overall simulated precipitation characteristics because non-convective precipitation characteristics (including its F, I, and D) are closer to observed values than those of convective precipitation (Chen & Dai, 2019). Unlike GCMs, observational products classify convective and non-convective precipitation by radar reflectivity (Awaka et al., 1997). This leads to differences in how observations and models define the convective-to-total precipitation (PC/PR) ratio. Despite this inconsistency, this ratio still provides a useful metric for evaluating GCMs. Bacmeister et al. (2014) showed that the PC/PR ratio in the tropics is considerably higher in CAM than in TRMM satellite observations, which is estimated to be around 0.5 (Dai, 2006; Yang & Smith, 2008). This ratio decreases as model grid spacing decreases (Bacmeister et al., 2014; Chen & Dai, 2019), because more precipitation is resolved by microphysics schemes and less is parameterized by cumulus schemes with smaller grid sizes. Increasing model resolution also improves the simulation of extreme precipitation (Kopparla et al., 2013; Wehner et al., 2014;). Therefore, increasing model resolution and/or reducing parameterized convective precipitation (e.g., Arakawa & Wu, 2013) could help reduce the "drizzling" bias.

The above studies are mostly based on a few individual models (mainly CAM) or CMIP3 models. It is worthwhile to investigate whether these results apply to other recent climate models. Many CMIP5 models also suffer from the "drizzling" bias (Flato et al., 2013). The CMIP5 models differ considerably from each other in many aspects, such as resolution and precipitation schemes; these factors have substantial influences on their simulated precipitation (Benedict et al., 2017; Covey et al., 2016; O'Brien et al., 2013). In particular, the moist convection and microphysics schemes that directly produce precipitation differ considerably (Rosa & Collins, 2013). Increasing model resolution likely improves the simulated precipitation characteristics for individual models (Chen & Dai, 2019; Kopparla et al., 2013). However, it is impractical to vary the resolution of each GCM to investigate this effect. Nevertheless, it may be informative to group the CMIP5 models into

a few categories, according to their resolution or formulations of certain physics processes (e.g., DeAngelis et al., 2015; Rosa & Collins, 2013; Thackeray et al., 2018).

Building on the CAM-based results of Chen and Dai (2019), here we address the "drizzling" problem in CMIP5 models. We start from the perspective of precipitation partitioning (i.e., the PC/PR ratio), and suggest ways to improve the simulated precipitation characteristics. Specifically, we investigate (a) whether the PC/PR ratio is too high in the CMIP5 and CMIP6 models with different types of parameterizations; (b) whether biases in the PC/PR ratio and convective precipitation contribute to the "drizzling" bias for total precipitation, and (c) whether model resolution also plays a role in these biases. We also analyze several CMIP6 models to find out whether this bias has been reduced in the new generation of models.

2. Data and Methods

2.1. CMIP Models and Their Classification

We use three-hourly data of total and convective precipitation for 1980–2005 from the all-forcing historical simulations done by 25 CMIP5 models and 6 CMIP6 models (Table 1). Non-convective precipitation is calculated by subtracting convective precipitation from total precipitation. Also listed in Table 1 are the models' horizontal grid spacing, and deep convection and large-scale (i.e., non-convective) precipitation schemes.

As shown in Table 1, various deep convection and microphysics schemes were employed in the models. To provide some physical guidance in evaluating precipitation, we classified the GCMs mainly based on their convective parameterizations (see Table 1). Many models used mass flux-type schemes such as the Arakawa and Schubert (1974, hereafter "AS") and ZM95. For cloud microphysics schemes, several models adopted the Rasch and Kristjánsson (1998, hereafter RK98) and Tiedtke (1993) schemes. A detailed description of these schemes is beyond the scope of this study.

By classifying the GCMs into nine groups, each with similar convection schemes and often also similar microphysics schemes (Table 1), we hope to gain physical insights during the evaluation. For instance, many of the models in the "ZM" group, which includes models that use the ZM95 scheme, also use the RK98 microphysics scheme. The "AS" group is for models whose convective parameterizations are based on the AS scheme, and three of five such models use the Le Treut and Li (1991) microphysics scheme. Of course, even models with the same parameterizations may have their own nuances; likewise, different parameterizations might be similar in certain ways. Nonetheless, we hope that such a classification can help us understand the influence of the schemes on precipitation partitioning and the "drizzling" bias.

2.2. Observational Datasets and Metrics Calculation

We used 3-hourly precipitation on a 0.25° grid from 50°S to 50°from TRMM satellite observations, namely TRMM 3B42 data set (TRMM, 2011a), to evaluate the model simulations. TRMM 3B42 3-hourly precipitation estimates were adjusted to match the monthly rain-gauge-based analysis from GPCP (Huffman et al., 2007). The spatial patterns of the mean precipitation amount in TRMM 3B42 are comparable to other observational products (Dai et al., 2007). Another TRMM product, 3A25 (TRMM, 2011b), classifies monthly precipitation (on a 0.5° grid from 45° to 45°N) into three categories: stratiform, convective, and other (a small part, added to total precipitation) by a vertical profile method (V-method) and a horizontal pattern method (H-method, Awaka et al., 1997; Yang & Smith, 2008). We used the convective and total monthly precipitation from TRMM 3A25 to derive the PC/PR ratio as an approximate reference for evaluating model-simulated PC/PR ratio. We realize that the definition of convective precipitation is not exactly the same between TRMM 3A25 and CMIP5 models (Dai, 2006; Pendergrass & Hartmann, 2014). Thus, the TRMM-based PC/PR ratio is used only as a rough estimate in this comparison. GPCP v2.2 (Huffman et al., 2009) monthly precipitation is used as a sanity check of the simulated precipitation amount.

The PC/PR ratio is calculated using multi-year (1980–2005 for models, 1998–2014 for TRMM) mean convective precipitation and total precipitation at each grid point. The calculation of precipitation characteristics follows our previous studies (e.g., Dai, 2006; Chen & Dai, 2019). To define non-trace 3-hourly precipitation (P), we used the threshold of $P > 0.1$ mm/hr as in Dai et al. (2007). Precipitation frequency is the number of 3-hourly precipitation events divided by the total number of observations or samples, intensity is the mean

Table 1
*Twenty-Five CMIP5 and Six CMIP6 (Marked by *) Models, Their Grid Size, Deep Convection, and Large-Scale Precipitation Schemes*

Group name (group-averaged PC/PR, F, I, and D)	Model name (PC/PR, F, I, and D)	Atmospheric grid size (lat x lon)	Deep convection scheme	Large-scale precipitation scheme
ZM (0.79, 28.86, 0.55, 15.55)	CCSM4 (0.76, 34.03, 0.46, 26.84)	~1.25° × 0.94°	Mass-flux scheme, (Zhang and McFarlane, 1995)	Rasch and Kristjánsson (1998); Zhang et al. (2003)
	NorESM1-M (0.79, 35.20, 0.40, 15.46)	~2.5° × 1.9°	Same as above	Same as above
	bcc-csm1-1 (0.86, 22.48, 0.64, 11.86)	~2.8° × 2.8°	Zhang and McFarlane (1995); Zhang (2002); Zhang and Mu (2005)	
	FGOALS-g2 (0.72, 19.2, 0.76, 8.61)	~2.8° × 3°	Same as above	
	BNU-ESM (0.93, 39, 0.40, 9.89)	~2.8° × 2.8°		
	bcc-csm1-1-m (0.69, 23.24, 0.64, 20.64)	~1.125° × 1.125°	Similar to above; Wu (2012)	
AS (0.67, 26.18, 0.58, 11.65)	MIROC5 (0.69, 31.6, 0.49, 12.6)	~1.4° × 1.4°	Entraining plume, based on Gregory (2001) and Arakawa and Schubert (1974); Chikira and Sugiyama (2010)	Wilson and Ballard (1999); Watanabe et al. (2010)
	MIROC-ESM (0.76, 28.31, 0.51,14.07)	~2.8° × 2.8°	Arakawa and Schubert (1974); (Emori et al., 2001)	Watanabe et al. (2011)
	MIROC-ESM-CHEM (0.77, 28.43, 0.51, 14.12)	~2.8° × 2.8°	Same as above	Same as above
	MIROC4h (0.47, 19.2, 0.78, 8.5)	~0.56° × 0.56°		
	MRI-CGCM3 (0.67, 23.38, 0.61, 8.94)	1.125° × 1.125°	mass-flux, based on Arakawa and Schubert (1974) and Tiedtke (1989); Yukimoto et al. (2012)	Based on Tiedtke (1993); MRI-TMBC scheme (2012)
	*MIROC6 (0.78, 27.36, 0.58, 11.93)	~1.4° × 1.4°	Same as MIROC5, Tatebe et al. (2019)	Same as MIROC5, Tatebe et al. (2019)
GFDL (0.93, 34.21, 0.45, 28.55)	GFDL-ESM2G (0.95, 33.67, 0.46, 29.67)	2.5° × 2.0°	Relaxed Arakawa-Schubert scheme, Moorthi and Suarez (1992)	Anderson et al. (2004)
	GFDL-ESM2M (0.96, 33.97, 0.44, 28.68)	2.5° × 2.0°		
	GFDL-CM3 (0.88, 34.98, 0.44, 27.3)	2.5° × 2.0°	Donner et al. (2011); Wilcox and Donner (2007)	Same as above
	*GFDL-CM4 (0.68, 29.34, 0.50, 21.57)	2.5° × 2.0°	Zhao et al. (2018)	Same as above
Tiedtke (0.85, 21.60, 0.73, 8.88)	CMCC-CM (0.75, 17.05, 0.91, 9.14)	0.75° × 0.75°	Mass flux scheme, Tiedtke (1989); Nordeng (1994)	Lohmann and Roeckner (1996)
	FGOALS-s2 (1.00, 19.17, 0.79, 7.47)	~2.8° × 1.7°	Mass flux scheme, Tiedtke (1989)	Bao et al. (2013)
	EC-EARTH (0.79, 28.59, 0.49, 10.04)	1.125° × 1.125°	Tiedtke (1989); Bechtold et al. (2008)	Tiedtke (1993)
	*EC-Earth3 (0.81, 31.84, 0.58, 9.67)	~0.70° × 0.70°	Same as above, Massonnet et al. (2020)	Massonnet et al. (2020)
UK (0.86, 25.83, 0.58, 11.64)	HadGEM2-ES (0.97, 23.93, 0.63, 12.04)	~1.875° × 1.24°	Mass-flux scheme, Gregory and Rowntree (1990)	Smith (1990); Wilson and Ballard (1999)
	ACCESS1-3 (0.74, 27.73, 0.52, 11.23)	~1.9° × 1.25°	Same as above, Bi et al. (2013)	Same as above

Table 1
Continued

Group name (group-averaged PC/PR, F, I, and D)	Model name (PC/PR, F, I, and D)	Atmospheric grid size (lat x lon)	Deep convection scheme	Large-scale precipitation scheme
GISS (0.48, 31.53, 0.57, 13.28)	GISS-E2-H (0.48, 29.72, 0.57, 13.34)	2.5° × 2.0°	Yao and Del Genio (1989); Gregory (2001)	Del Genio et al. (1996); Schmidt et al. (2014)
	GISS-E2-R (0.48, 33.34, 0.56, 13.21)	2.5° × 2.0°	Same as above	Same as above
	*GISS-E2-1-G (0.39, 24.40, 0.63, 17.82)	2.5° × 2.0°	Kelley et al. (2020)	Kelley et al. (2020)
Emanuel (0.73, 32.65, 0.45, 20.31)	IPSL-CM5A-LR (0.74, 32.47, 0.43, 20.13)	~3.75° × 1.875°	Mass-flux scheme, Emanuel (1991)	Le Treut and Li (1991); Hourdin et al. (2006)
	IPSL-CM5A-MR (0.72, 32.83, 0.46, 20.49)	~2.5° × 1.25°	Same as above	Same as above
	*IPSL-CM6A-LR (0.82, 40.24, 0.40, 51.25)	~2.5° × 1.25°	Hourdin et al. (2020)	Hourdin et al. (2020)
	CNRM-CM5 (0.94, 37.22, 0.47, 12,74)	~1.4° × 1.4°	Bougeault (1982)	Ricard and Royer (1993)
	*CNRM-CM6 (0.58, 20.57, 0.75, 12.88)	~1.4° × 1.4°	Voldoire et al. (2019)	Voldoire et al. (2019)
	INMCM4 (0.95, 50.83, 0.34, 47.79)	2.0° × 1.5°	Betts (1986)	Diagnostic calculation of cloud fraction

Note. The four values in parentheses following each model group name are the mean PC/PR ratio, F (%), I (mm/hr) and D (hr) in the tropics (20°S–20°N) for the group, while the values following each model name are the same metrics for the model.

Abbreviations: CMIP5, Climate Model Intercomparison Project Phase 5; PC/PR, convective-to-total precipitation

precipitation rate averaged over all precipitation events ($F \times I = A / \Delta t$, where A is accumulated precipitation, and Δt is the time of accumulation), and duration is the temporal length of a continuous precipitation event at a given grid during which the rates exceed the 0.1 mm/hr threshold for all the 3-h periods. It is worth mentioning that the F, I and D are sensitive to the thresholds chosen (e.g., Trenberth Zhang, 2018; Chen & Dai, 2018), with higher threshold values yield lower F and D but higher I. However, because the same threshold is applied to all models and observations, the afore-mentioned sensitivity does not affect the general results. The F, I, and D are computed at each grid box for each season of each year and then averaged over all the years. Lastly, model grid spacing is measured using $\Delta = \sqrt{\Delta x \Delta y}$, with Δx (°) and Δy (°) being the meridional and zonal grid spacing in degrees. The Δr ranges from ~0.5° to ~2.9° for the CMIP5 models. Note that instead of interpolating models to a common grid, we used data on their native grid to calculate the F, I, and D. We did so because all spatial interpolations of precipitation would inevitably change the probability of precipitation, and hence affect the estimated characteristics (Chen & Dai, 2018). For comparing with model F, I, and D, we simply averaged the TRMM 3B42 3-hourly precipitation data onto 0.5° lat × 0.5° lon, 1.0° × 1.0°, 1.5° × 1.5°, 2.0° × 2.0°, 2.5° × 2.5°, and 3.0° × 3.0° grids, so that one of these grids is close to a model grid. Using data with similar spatial and temporal resolution is critical for comparing these precipitation characteristics, because their estimated values are highly sensitive to the data resolution (Chen & Dai, 2018).

3. The PC/PR Ratio and Precipitation Characteristics in CMIP5 Models

Despite simulating fairly realistic precipitation amounts (not shown), the PC/PR ratio between 20°S and 20°N is well above the TRMM satellite estimate of ~0.45 in all 25 CMIP5 models (Figure 1, Table 1). This was also the case in CMIP3 models (Dai, 2006) and CAM (Chen & Dai, 2019). FGOALS-s2 has a PC/PR ratio of 1.0 (i.e., no non-convective precipitation) between about 50°S and 30°N (Figure 1). Hence, we consider FGOALS-s2 as an outlier and excluded it in subsequent analyses. The PC/PR ratio has little variation within 20°S–20°N for individual models, but decreases rapidly outside the tropics. The high PC/PR ratio

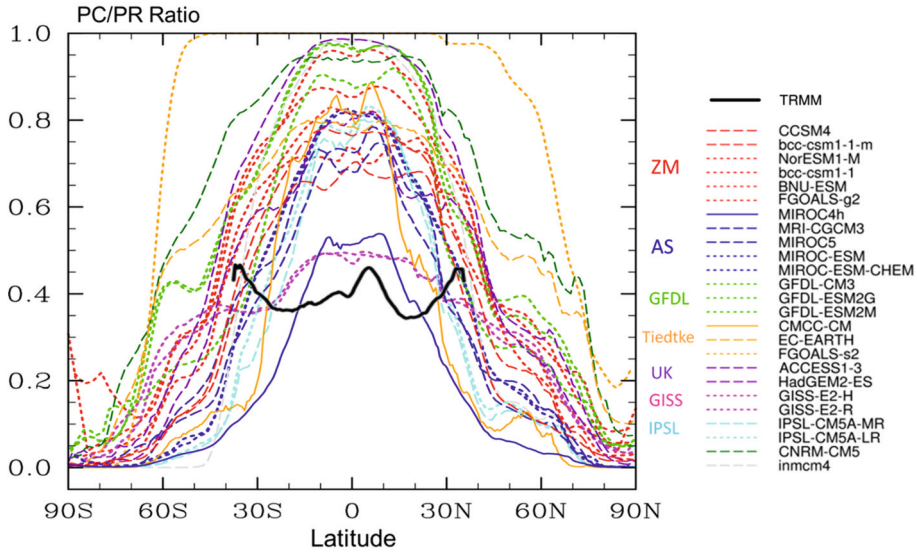

Figure 1. The convective-to-total precipitation (PC/PR) ratio as a function of latitude in TRMM 3A25 (0.5°, thick black line) and 25 Climate Model Intercomparison Project Phase 5 (CMIP5) models. Models are color-coded and annotated by the parameterization type groups (see Table 1). Line patterns differ for models with different resolution: solid lines are for models with <1.0° grid sizes, dash lines are for 1.0°–2.0° and dotted lines are for >2.0° models.

in most CMIP5 models indicates that convective parameterizations may be overly active in producing convective precipitation, particularly at low latitudes. By grouping models by their convective and microphysics schemes, and comparing them on different spatial resolution within the same parameterization group (shown in same line color), we attempt to understand the separate influence of model resolution and physical schemes. The group-averaged PC/PR ratio, F, I, and D also suggest that the various parameterization types (Table 1) do not produce substantially different precipitation partitioning. Within the same group, the PC/PR ratio is smaller in models on finer resolution. This is mostly evident for the AS and Tiedtke groups, which include grid spacing from ~0.5° to 2.8°. Yet this effect differs among different groups, and more rigorous sensitivity experiment (e.g., Chen & Dai, 2019) is required for confirmation.

Next, we select one model from each parameterization group (with similar grid spacing within 1°–2° when available) to illustrate model biases in precipitation characteristics (Figure 2). For total precipitation, most models have higher F and D, but lower I than TRMM (Figures 2a–2c). Note that the selected models all have grid spacing smaller than 2.5°. But even compared with the 2.5° TRMM benchmark, the bias is still considerable. Over the tropics, the range of F is 30%–50% in the models, while it is 20%–30% in the 2.5° TRMM. Meanwhile, TRMM values are even smaller on a 0.5° grid. The overestimation is also striking for duration: models typically yield durations of 10–40 h, while TRMM observations are mostly below 10 h. Precipitation is less intense in the models than in real world, typically being only half the observed magnitude. The opposite is true for frequency. Overall, there are no obvious differences among parameterization types in terms of capturing the observed characteristics. Among them, MIROC5, EC-EARTH, HadGEM2-ES, and GISS-E2-R have relatively moderate "drizzling" bias. In most panels of Figure 2, the former three models have lower frequency, higher intensity, and shorter duration of precipitation events, which are closer to TRMM's values. For GISS-E2-R, it is worth noting that its convective and non-convective precipitation do not differ much in their characteristics. Both components exhibit moderate "drizzling" bias, leading to slightly larger "drizzling" bias than the other three models for its total precipitation.

Chen and Dai (2019) found that convective precipitation in CAM is more frequent and long-lasting, but less intense than non-convective precipitation. Overall, this is also true for many CMIP5 models in low latitudes (Figure 2). The frequency is substantially higher for convective precipitation than for non-convective precipitation (Figures 2d and 2g). Some models have a frequency of <5% for non-convective precipitation in low latitudes (Figure 2g). The differences are less clear for intensity (Figures 2e and 2h). Four models (CCSM4, GFDL-CM3, CNRM-CM5, and GISS-E2-R) have higher intensity for non-convective than for

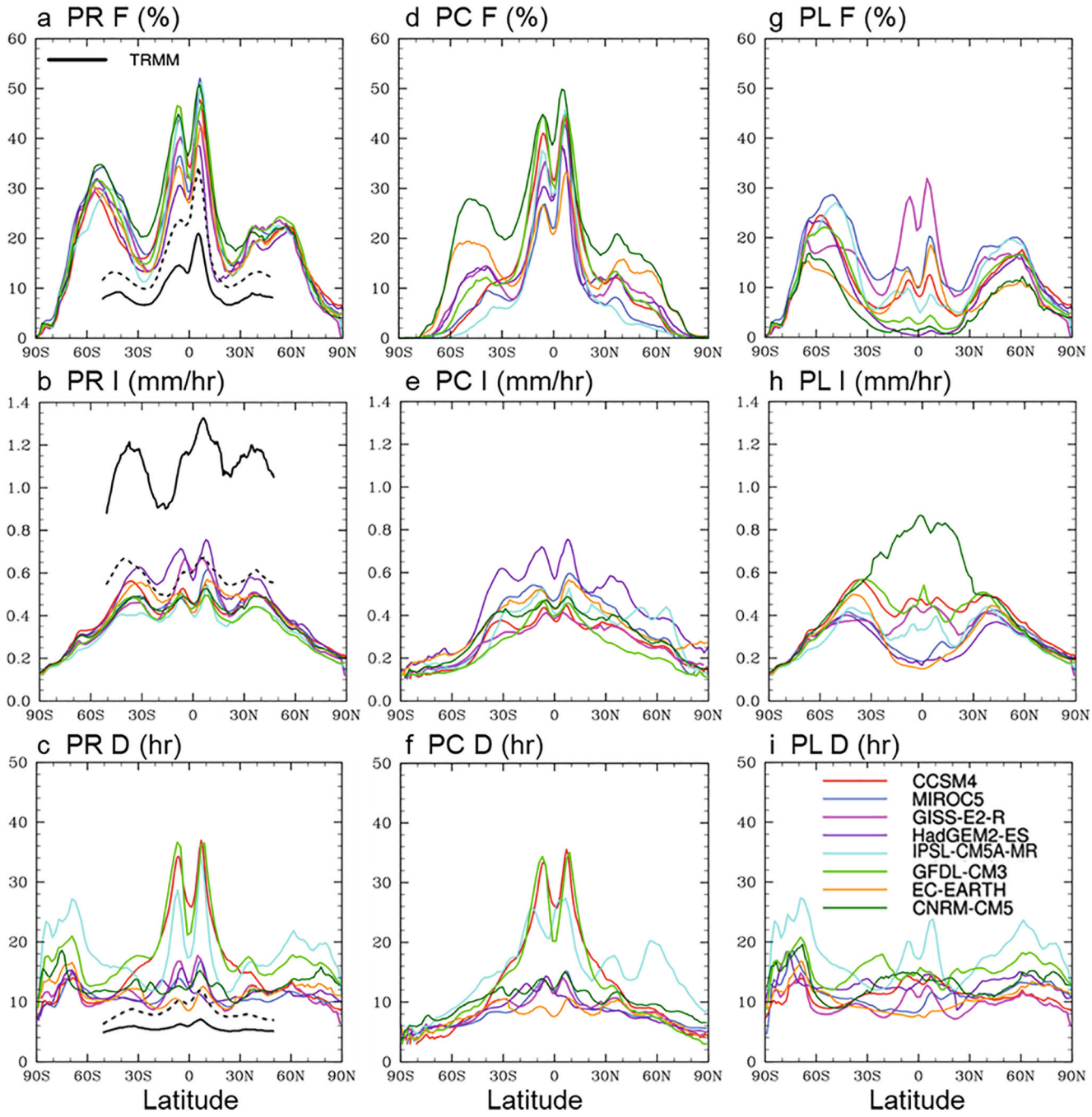

Figure 2. Zonal-mean (a, d and g) frequency (F, %), (b, e and h) intensity (I, mm/hr) and (c, f and i) duration (D, hours) for total (PR, left), convective (PC, middle) and non-convective precipitation (PL, right) as a function of latitude. Eight models (CCSM4 (red), MIROC5 (blue), GISS-E2-R (magenta), HadGEM2-ES (purple), IPSL-CM5A-MR (cyan), GFDL-CM3 (lightgreen) EC-EARTH (orange), and CNRM-CM5 (darkgreen)) using different convective parameterization schemes and closest resolution (see Table 1) are shown here. Values from TRMM 3B42 (thick black line for data on 0.5° grid and dash black line for data on 2.5° grid) are plotted for comparison.

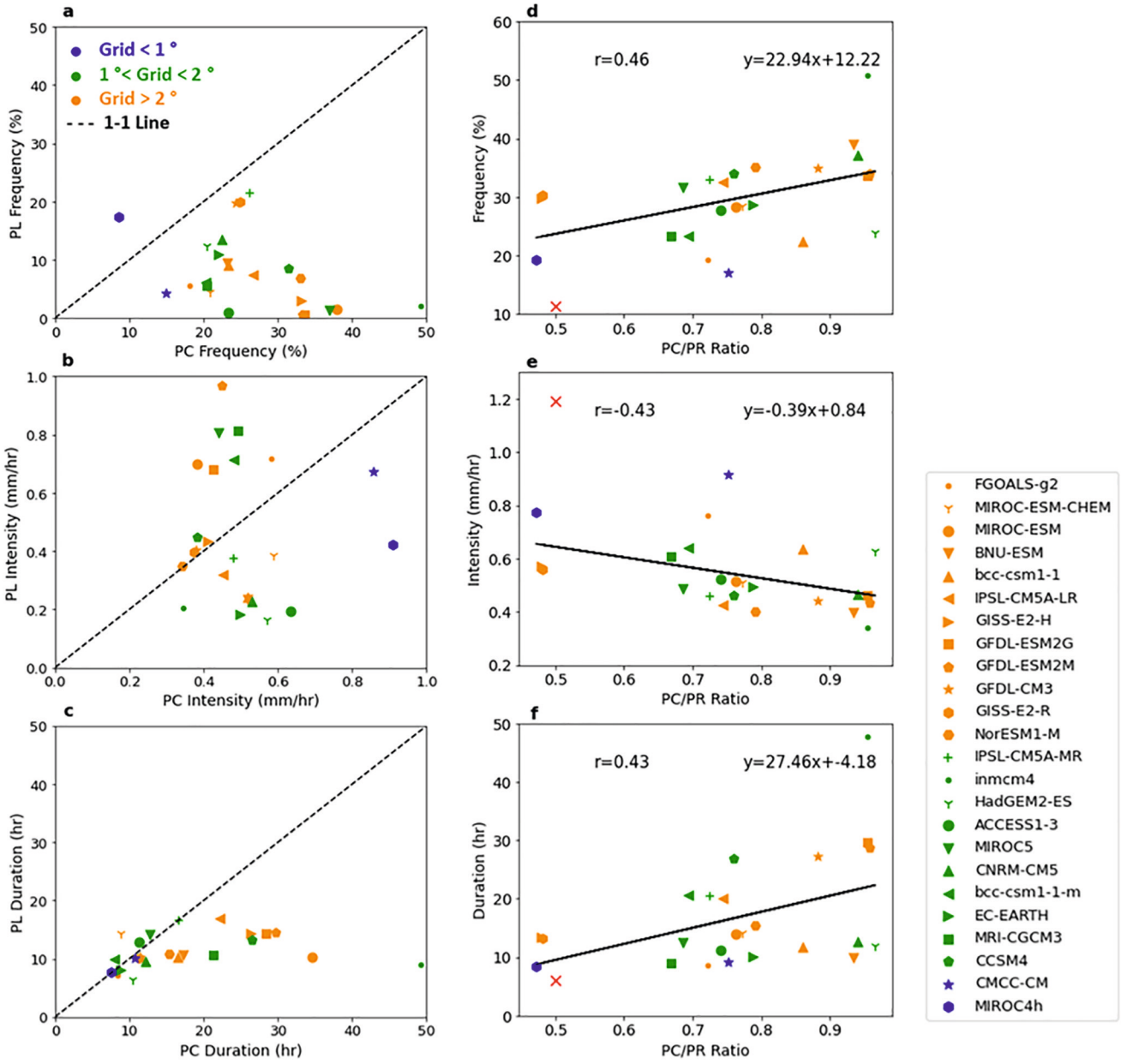

Figure 3. (Left, a–c) Scatter plots of tropical (20°S–20°N) mean frequency (F, %), intensity (I, mm/hr), and duration (D, hr) for convective (PC, *x*-axis) and non-convective (PL, *y*-axis) precipitation; and (Right, d–f) tropical (20°S–20°N) mean F, I, and D for total precipitation as a function of convective-to-total precipitation (PC/PR) ratio for the 24 Climate Model Intercomparison Project Phase 5 (CMIP5) models. Model grid spacings are color coded as shown on panel (a). Linear regression lines and equations are shown in black. TRMM values (0.5° grid) are also shown (red cross).

convective precipitation, while three others (HadGEM2-ES, MIROC5, and EC-EARTH) show lower intensity for non-convective precipitation. However, all models agree that tropical convective precipitation lasts longer than non-convective precipitation (Figures 2f and 2i).

4. Linking the PC/PR Ratio to the "Drizzling" Bias

The above results show that the "drizzling" bias is most prominent over the tropics (20°S–20°N). Hence, we focus on this region in the following analyses. First, we check whether convective and non-convective precipitation show different characteristics over the tropics across the 24 models. In the tropics, convective precipitation shows higher frequency (Figure 3a) and duration (Figure 3c) than non-convective precipitation

in most models. For intensity, models with >1° grid spacing exhibit mixed results, while the two models (MIROC4h and CMCC-CM) with <1° grids show higher intensity for convective than non-convective precipitation (Figure 3b). Surprisingly, the F, I, and D for the PC and PL only show a weak dependence on model resolution among the 24 CMIP5 models (Figures 3a–3c). Some models with <2° grids even have higher PC frequency than >2° grids models, while some models with >2° grids show higher PL intensity than models with <2° grids. This is in contrast to what is seen in CAM4, in which the F and D of PC increases greatly with grid size while the I of PL decreases rapidly with grid size (Chen & Dai, 2019). This suggests that differences in CMIP5 model physics are as important (if not more) as their resolution differences, in determining the precipitation characteristics.

The systematic F and D differences between convective and non-convective precipitation, together with the dominance of convective precipitation over the tropics, led us to hypothesize that the high PC/PR ratio may be related to the "drizzling" bias in low latitudes. Figures 3d–3f show the tropical-mean F, I, and D of total precipitation as a function of the PC/PR ratio across the 24 models. Overall, higher PC/PR ratios are associated with larger F and D but weaker I, although the data points are more scattered for higher PC/PR ratios. The PC/PR ratio is significantly correlated with the F, I, and D (correlation coefficients are 0.46, −0.43, and 0.43, respectively). We did a sensitivity test by removing the two GISS models, because their PC/PR ratio is much lower than other models with similar gird spacings. The correlation between the PC/PR ratio and F, I, and D (0.58, −0.5, and 0.46, respectively) further strengthens. These results suggest a link between the PC/PR ratio and the "drizzling" bias among the CMIP5 models, such that models with higher PC/PR ratios typically have more severe "drizzling" biases. As shown in Figures 3a–3c, convective precipitation is usually more frequent and long-lasting. The results for intensity are mixed, with about 12 models have more intense non-convective precipitation than convective precipitation, while the other 12 models show the opposite. Interestingly, the two models with <1° gird show higher intensity for convective precipitation than for non-convective precipitation. Figure 3b shows that convective precipitation overall has lower intensity than non-convective precipitation among the CMIP5 models, consistent with CAM-based results (Chen & Dai, 2019). A high PC/PR ratio in a particular model means that total precipitation tends to inherit more characteristics of convective precipitation than non-convective precipitation, leading to a more severe "drizzling" bias.

Previous studies also showed that the estimated precipitation characteristics are sensitive to data or model resolution, and model resolution also influences partitioning of total precipitation for a given model (Chen & Dai, 2018; 2019). Figure 4 shows the PC/PR ratio, F, I, and D for total precipitation as a function of the model grid spacing. Overall, the dependence of F, I, and D on resolution shown in Figures 4b–4d are weaker than their dependence on the PC/PR ratio shown in Figures 3d–3f, again likely due to large influences from different model physics. For grid spacing within 0.5°–2.0°, higher-resolution models (especially CMCC-CM and MIROC4h) generally have lower PC/PR ratios, frequency, and duration, but higher intensity than coarser-resolution models (Figure 4). However, this dependence weakens when the grid spacing is within 2.0°–3.0°, over which the dependence of the intensity on grid size also weakens in the TRMM data (Figure 4). In fact, when computing the correlation among models with grid spacing <2° and >2° separately (Figure S1), the relationships are reversed. A few models (namely FGOALS-g2 and bcc-csm1-1) with the grid sizes around 3.0° have values similar to models with the highest resolution. This leads to the overall weaker dependence of precipitation characteristics on resolution across all models. Removing these two models boosts the correlation to 0.45 and −0.59 (p-value < 0.05) for frequency and intensity, but the correlation coefficients for the PC/PR ratio and duration still remain insignificant (Figure S2). The relatively weak dependence on resolution among the CMIP5 models is expected given the large differences in cumulus schemes and other model physics among them, which all can contribute to the differences in their precipitation characteristics. This is in contrast to the case where one model is used and the main difference is the grid spacing, whose influence on precipitation characteristics is much stronger (Chen & Dai, 2019).

To find out whether the weak dependence above 2° is due to a diminishing area-aggregation (as the spatial sampling area or the size of grid box increases, the probability or frequency of precipitation increases, meanwhile intensity decreases, see Chen & Dai, 2018) effect, TRMM estimates on different grids and fitted relationships are also shown in Figure 4. The F and D still increase linearly above 2°, while intensity decreases roughly exponentially with resolution. This suggests that the area-aggregation effect above 2° does

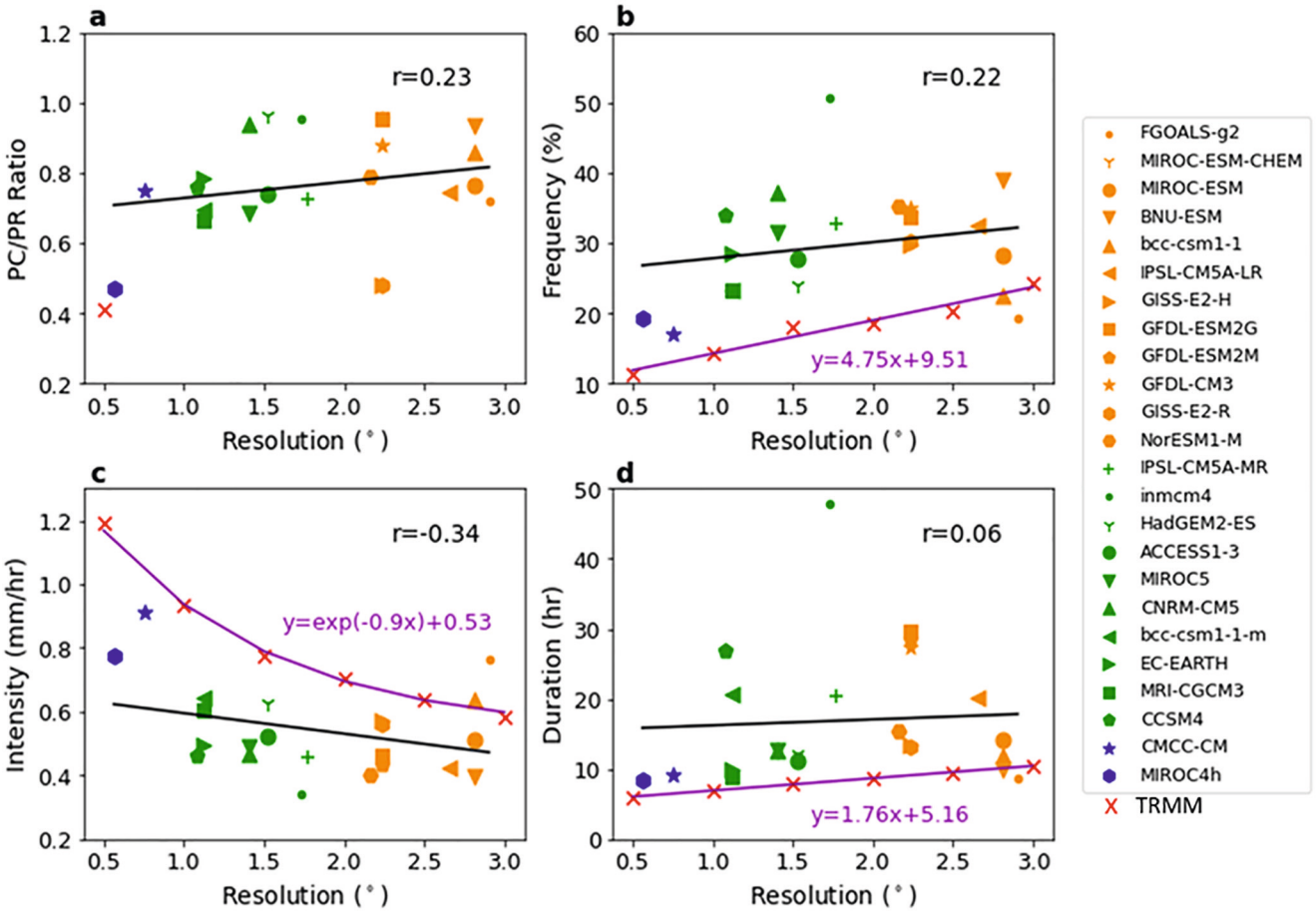

Figure 4. Tropical (20°S–20°N) mean (a) convective-to-total precipitation (PC/PR) ratio, (b) frequency (F, %), (c) intensity (I, mm/hr) and (d) duration (D, hr) of total precipitation as a function of model grid sizes for the 24 CMIP5 models. Annotations are same as Figure 3. The TRMM PC/PR ratio (0.5°) and the F, I, and D (on 0.5°, 1.0°, 1.5°, 2.0°, 2.5°, and 3.0° grids, red cross) and fitted functions (purple) are also shown.

not diminish for the F and D, but notably weakens for intensity. While other models with >2.0° resolution still have large biases, two models with the lowest resolutions (i.e., FGOALS-g2 and bcc-csm1-1) have modest "drizzling" bias. When removed them, the correlation coefficients between grid spacing and the F and I become significant (0.45 and −0.59), but not for duration. Thus, it is likely that overall the area-aggregation effect is overshadowed by the influence of different model physics for models with >2.0° grid spacing, leading to no clear dependence of the F, I, and D on their model resolution.

Figure 5 summarizes the inter-model correlation coefficients among model resolution, PC/PR ratio, frequency, intensity, and duration for the 24 CMIP5 models. Higher PC/PR ratio is associated with higher F, D but lower I, and vice versa. The correlations between model resolution and the other variables are statistically insignificant, and weaker than the correlations with the PC/PR ratio, especially for duration (Figure 5). Because PC/PR ratio is weakly related to resolution (Figure 4a), we then calculated partial correlation coefficients by removing the influence of resolution through linear regression. The partial correlation between the PC/PR ratio and F or D is still significant at a 0.05 significance level. For intensity, the partial correlation is significant at a 0.1 significance level. Therefore, adjusting the partitioning of total precipitation, for example, by modifying the convective and microphysics schemes to reduce convective precipitation while increasing non-convective precipitation (without increasing resolution) could reduce the "drizzling" bias. Another approach is to increase resolution for individual models, as more non-convective precipitation would be resolved while less precipitation is convectively parameterized. The latter typically requires more computing power. Note that the correlations are strong among the F, I, and D since they are interrelated characteristics of precipitation.

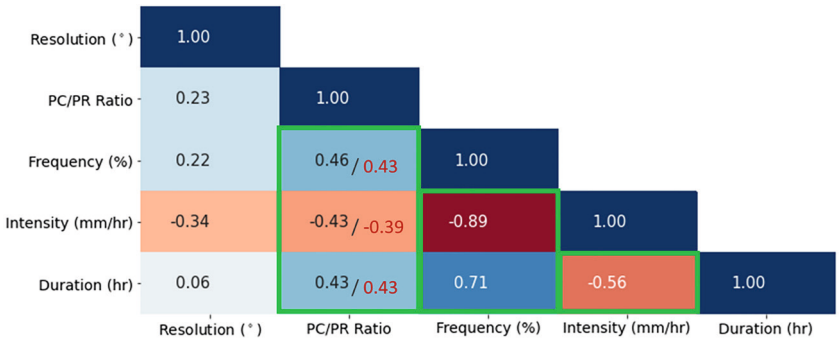

Figure 5. Cross correlation coefficients of model resolution, convective-to-total precipitation (PC/PR) ratio, precipitation frequency, intensity, and duration among the 24 Climate Model Intercomparison Project Phase 5 (CMIP5) models. Partial correlation coefficients between the PC/PR ratio and F, I, or D are shown in red calculated by removing the effect of resolution. The correlation coefficients that are significant at least at a 10% significance level are contained in the green rectangles.

The release of CMIP6 offers an opportunity to explore whether the "drizzling" bias has been alleviated in new versions of these GCMs. For comparison, we examined changes in the "drizzling" bias in six CMIP6 models corresponding to six of the model groups (Table 1), including the GFDL-CM4, EC-Earth3, MIROC6, IPSL-CM6A-LR, CNRM-CM6, and GISS-E2-1-G. Their spatial resolutions are mostly the same as their CMIP5 version, except that we interpolated the metrics for EC-EARTH (1.125°) to match the grid of EC-Earth3 (0.703°). Due to data availability at the time we performed the analysis, we did not include CESM2 and HadGEM3 models. Figure 6 shows the difference of F, I, and D for total, convective, and non-convective precipitation between the 6 CMIP6 models and their CMIP5-version. A few models show overall decreased frequency and increased intensity compared with their predecessors (Figure 6). In particular, GFDL-CM4 and CNRM-CM6 exhibit appreciably reduced "drizzling" bias. The frequency for total and convective precipitation decreases about 10% over the tropics, while for non-convective precipitation it increases for up to 20% at 10°N for these two models. GFDL-CM4 also shows notable decrease of duration (Figures 6c and 6f). Other models show no clear improvement. With increased F and D, IPSL-CM6A-LR has a more severe bias than its CMIP5 version. To understand whether changes of the bias are related to PC/PR ratio in the 6 CMIP6 models, Figure 7a shows the difference of the PC/PR ratio between the CMIP6 and CMIP5 versions. Most noticeably, the PC/PR ratio decreases at every latitude in GFDL-CM4 and CNRM-CM6, whereas it generally increases in IPSL-CM6A-LR. Figure 7b further shows that models with larger decreases in tropical PC/PR ratio (e.g., CNRM-CM6 and GFDL-CM4) tend to have lower F and higher I, that is, reduced "drizzling" bias in the tropics. This inter-version comparison supports the results based on the CMIP5 models, and further suggests that more realistic precipitation partitioning between convective and non-convective precipitation helps alleviate the "drizzling" bias.

5. Summary and Discussion

We have analyzed 3-hourly precipitation from 24 CMIP5 models and 6 CMIP6 models to examine the partitioning between convective and non-convective precipitation, and how this partitioning is linked to the "drizzling" bias in the models. We found that most CMIP5 models have unrealistically high convective-to-total precipitation (PC/PR) ratio, and they all have the "drizzling" bias to different degrees, similar to CMIP3 models (Dai, 2006). We also found that convective precipitation exhibits higher frequency (F) and longer duration (D) than non-convective precipitation, but lower intensity (I, for some models), consistent with previous results with CAM4 and CAM5 (Chen & Dai, 2019). Combined with the high PC/PR ratio, this contributes to the "drizzling" bias. Significant relationships are found between the PC/PR ratio and the F, I, and D, such that a larger "drizzling" bias in low latitudes is typically associated with a higher PC/PR ratio. Furthermore, we showed that across the 24 CMIP5 models, the PC/PR ratio and the "drizzling" bias increase as the grid size increases from 0.5° to 2.0°. However, this dependence becomes weak as the grid size increases from 2.0° to 3.0°, even though the area-aggregation effect does not diminish above 2.0°. This weakening is partly due to two outlier models with the largest grid spacing. It also suggests that differences

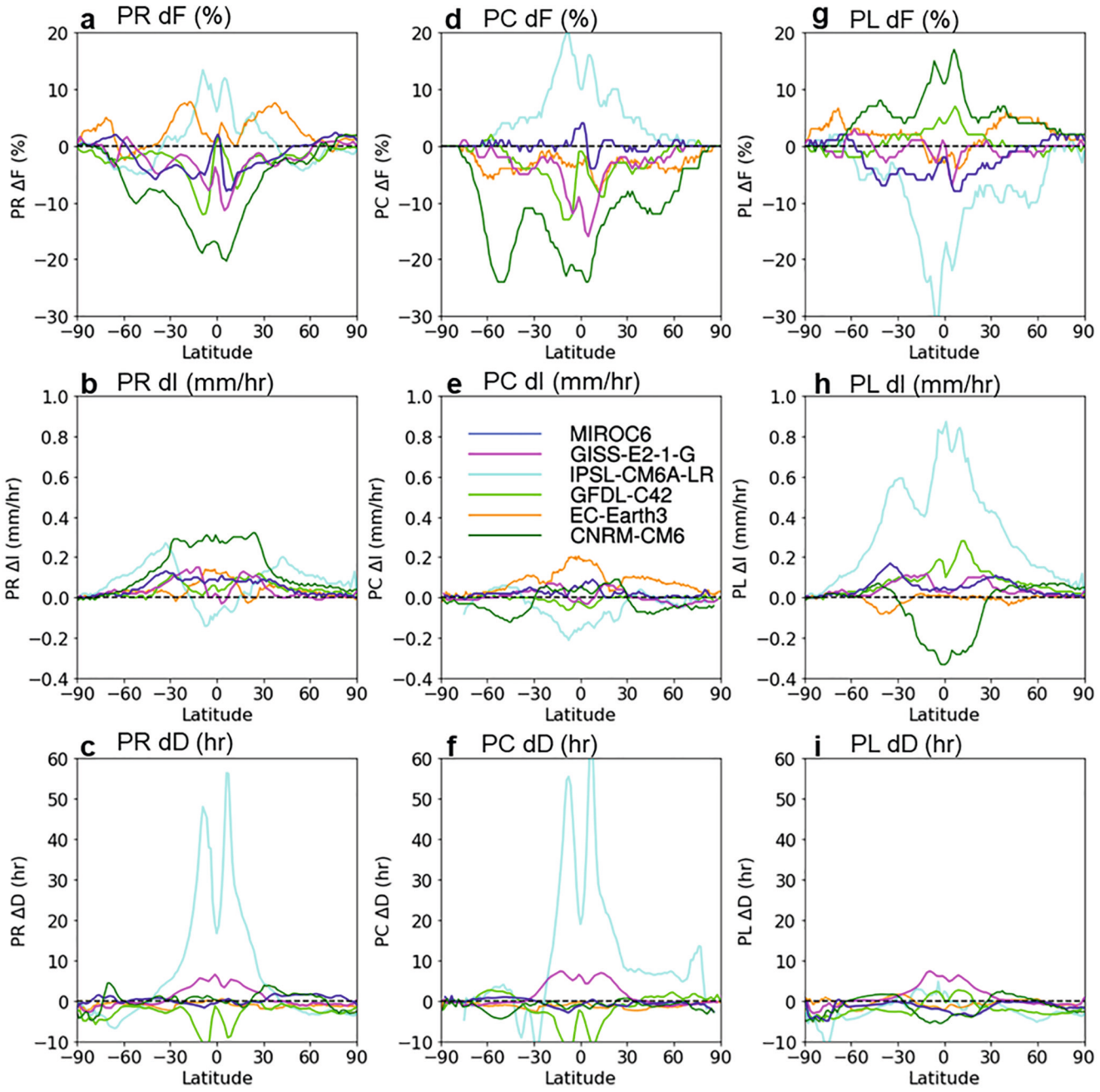

Figure 6. Difference of (a–c) total, (d–f) convective, and (g–i) non-convective precipitation characteristics between the Climate Model Intercomparison Project Phase 6 (CMIP6) and CMIP5 versions of six models. The CMIP6 models are MIROC6 (blue), GISS-E2-1-G (magenta), IPSL-CM6A-MR (cyan), GFDL-C42 (i.e., GFDL-CM4_gr2, lightgreen), EC-Earth3 (orange), and CNRM-CM6 (darkgreen).

in model physics play a bigger role at these resolutions. Different model physics also weaken the dependence on model resolution compared with that seen in a single model (Chen & Dai, 2019).

Nevertheless, tuning the precipitation schemes to reduce convective but increase non-convective precipitation should reduce the "drizzling" bias at low latitudes. Increasing model resolution also help in mitigating the biases. Some of the CMIP6 models show reduced "drizzling" bias associated with decreased PC/PR ratio. We believe the improved and more realistic precipitation partitioning in the six CMIP6 models (compared with their CMIP5 predecessors) contribute to the reduced "drizzling" bias. These results are generally consistent with previous findings that are mainly based on NCAR models (e.g., Chen & Dai, 2019).

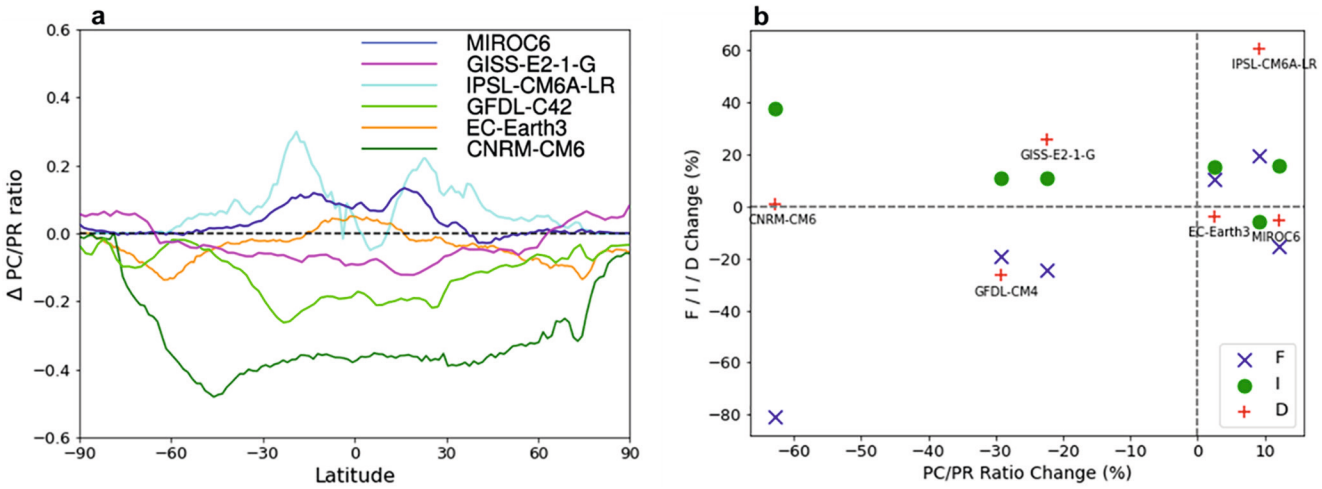

Figure 7. (a) Change of the convective-to-total precipitation (PC/PR) ratio as a function of latitude in 6 Climate Model Intercomparison Project Phase 6 (CMIP6) models. (b) Scatter plot showing relative change (%) of PC/PR ratio versus precipitation frequency (f), intensity (i) and duration (d), between the 6 CMIP6 models and their CMIP5 version. The CMIP6 models are MIROC6 (blue), GISS-E2-1-G (magenta), IPSL-CM6A-MR (cyan), GFDL-C42 (i.e., GFDL-CM4_gr2, lightgreen), EC-Earth3 (orange), and CNRM-CM6 (darkgreen).

Therefore, we recommend that besides the mean precipitation distributions in the tropics, the PC/PR ratio should be incorporated as a new metric for the modeling community to further improve precipitation simulation. Similar practices have been suggested by several previous studies (e.g., Bacmeister et al., 2014; Dai, 2006). We believe such metrics could allow more comprehensive diagnostics and evaluation in the model development process.

As mentioned above, the inconsistencies in the definition of the convective and non-convective precipitation between models and TRMM data make it difficult for a precise comparison. Some observational evidence indicates that convective precipitation intensity is smaller than that of stratiform precipitation over the vast oceans (Houze et al., 2015; Yang & Smith, 2008), similar to models' depictions. Over land, convective precipitation is more localized and can attain larger intensity than non-convective precipitation (Schumacher & Houze, 2003). However, the large PC/PR ratio difference over the tropics (Figure 1) between models and TRMM should exceed the uncertainty associated with the definition difference. Given these uncertainties, research efforts in unifying precipitation classification methods (e.g., Kay et al., 2018) would facilitate bridging the gap between observed and simulated precipitation.

In terms of the different parameterization groups, our results show that most of them have high PC/PR ratios and "drizzling" biases to different extent. Overall, there is no clear winner among the parameterization groups. The group-mean metrics (Table 1) suggest that models using Arakawa and Schubert (1974) and Tiedtke (1989) schemes appear to have a smaller "drizzling" bias. In the AS-type scheme, multiple convective updrafts with different heights (depending on the entrainment rate) are explicitly calculated within a single grid cell, although each updraft is a simplified entraining plume (Mizuta et al., 2012). Emanuel (1991) also pointed out that the quasi-equilibrium assumption in the AS scheme agrees with observations. In addition, most models in the AS group have a relative humidity (RH) threshold-based suppression mechanism, which prevents too frequent occurrence of convective precipitation (Rosa & Collins, 2013). On the other hand, only a single convective updraft is calculated within a single grid cell in the Tiedtke-type scheme, but more detailed entraining and detraining plume is represented. The resolution-dependent time scale for CAPE consumption, as in CMCC-CM (Nordeng, 1994), also helps adjust precipitation partitioning (Williamson, 2013) and reduce the "drizzling" bias. Two CMIP6 models (i.e., CNRM-CM6 and GFDL-CM4), which show reduced "drizzling" bias, used different convection schemes. A double plume convection scheme was used in GFDL-CM4. At a given time, the double plume scheme can contain one plume for shallow convection and another for deep convection (Zhao et al., 2018). CNRM-CM6 also contains major changes to its convection scheme over its CMIP5 version (Voldoire et al., 2019). In addition to continuous and prognostic treatment of dry, shallow, and deep convection, the new scheme separates convective

microphysical processes from convective scheme itself. The stratiform microphysics scheme is also changed from the one used in CNRM-CM5. These changes may play important roles in alleviating the "drizzling" bias in the two CMIP6 models. Hence, improved convection and microphysics schemes can lead to improved simulations of the precipitation characteristics, which adds credibility to their projections of future precipitation changes. Although our results show overall no salient difference among the parameterization groups, their nuances discussed above suggest that in-depth analyses from a moist process perspective might help pinpoint other key players (e.g., mean humidity and clouds) that lead to the differences. Better understanding of the biases in these key fields may shed light on the biases in precipitation partitioning and the "drizzling" bias across models that employ different physics parameterizations.

Data Availability Statement

CMIP5 model output is archived by PCMDI (available from https://pcmdi.llnl.gov/mips/cmip5). The TRMM 3B42 data set is available at https://disc.gsfc.nasa.gov/datasets/TRMM_3B42_7/summary?keywords=TRMM%203b42, and the TRMM 3A25 data set is available at https://disc.gsfc.nasa.gov/datasets/TRMM_3A25_7/summary?keywords=TRMM%203a25. The GPCP v2.2 is available at https://rda.ucar.edu/datasets/ds728.2/.

Acknowledgments
D. Chen and A. Hall were supported by the U.S Department of Energy's Regional and Global Climate Modeling Program under the project "Identifying Robust Cloud Feedbacks in Observations and Models. A. Dai was supported by the National Science Foundation (Award Nos AGS-2015780 and OISE-1743738), the US Department of Energy's Office of Science (DE-SC0012602) and the US National Oceanic and Atmospheric Administration (Award No NA18OAR4310425). We thank three reviewers whose constructive comments helped us improve the manuscript considerably.

References

Anderson, J. L., Balaji, V., Broccoli, A. J., Cooke, W. F., Delworth, T. L., & Garner, S. T. (2004). The new GFDL global atmosphere and land model AM2–LM2: Evaluation with prescribed SST simulations. *Journal of Climate*, *17*(24), 4641–4673. https://doi.org/10.1175/jcli-3223.1

Arakawa, A., & Schubert, W. H. (1974). Interaction of a cumulus cloud ensemble with the large-scale environment, part I. *Journal of the Atmospheric Sciences*, *31*, 674–701. https://doi.org/10.1175/1520-0469(1974)031<0674:IOACCE>2.0.CO;2

Arakawa, A., & Wu, C. M. (2013). A unified representation of deep moist convection in numerical modeling of the atmosphere. Part I. *Journal of the Atmospheric Sciences*, *70*(7), 1977–1992. https://doi.org/10.1175/JAS-D-12-0330.1

Awaka, J., Iguchi, T., Kumagai, H., & Okamoto, K. (1997). Rain type classification algorithm for TRMM precipitation radar. In *Geoscience and remote sensing*. IGARSS '97Remote sensing—A scientific vision for sustainable development (Vol. 4, pp. 1633–1635). New York: Institute of Electrical and Electronics Engineers. https://doi.org/10.1109/IGARSS.1997.608993

Bacmeister, J. T., Wehner, M. F., Neale, R. B., Gettelman, A., Hannay, C., Lauritzen, P. H., et al. (2014). Exploratory high-resolution climate simulations using the community atmosphere model (CAM). *Journal of Climate*, *27*(9), 3073–3099. https://doi.org/10.1175/JCLI-D-13-00387.1

Bao, Q., Lin, P., Zhou, T., Liu, Y., Yu, Y., Wu, G., et al. (2013). The flexible global ocean-atmosphere-land system model, spectral version 2: FGOALS-s2. *Advances in Atmospheric Sciences*, *30*(3), 561–576. https://doi.org/10.1007/s00376-012-2113-9

Bechtold, P., Köhler, M., Jung, T., Doblas-Reyes, F., Leutbecher, M., Rodwell, M. J., et al. (2008). Advances in simulating atmospheric variability with the ECMWF model: From synoptic to decadal time-scales. *Quarterly Journal of the Royal Meteorological Society*, *134*, 1337–1351. https://doi.org/10.1002/qj.289

Benedict, J. J., Medeiros, B., Clement, A. C., & Pendergrass, A. G. (2017). Sensitivities of the hydrologic cycle to model physics, grid resolution, and ocean type in the aquaplanet Community Atmosphere Model. *Journal of Advances in Modeling Earth Systems*, *9*, 1307–1324. https://doi.org/10.1002/2016MS000891

Betts, A. K. (1986). A new convective adjustment scheme. Part I: Observational and theoretical basis. *Quarterly Journal of the Royal Meteorological Society*, *112*(473), 677–691. https://doi.org/10.1002/qj.49711247307

Bi, D., Dix, M., Marsland, S. J., O'Farrell, S., Rashid, H., Uotila, P., et al. (2013). The ACCESS coupled model: Description, control climate and evaluation. *Australian Meteorological and Oceanographic Journal*, *63*, 41–64. https://doi.org/10.22499/2.6301.004

Bougeault, P. (1982). Cloud-ensemble relations based on the gamma probability distribution for the higher-order models of the planetary boundary layer. *Journal of the Atmospheric Sciences*, *39*(12), 2691–2700. https://doi.org/10.1175/1520-0469(1982)039<2691:cerbot>2.0.co;2

Chen, D., & Dai, A. (2018). Dependence of estimated precipitation frequency and intensity on data resolution. *Climate Dynamics*, *50*, 3625–3647. https://doi.org/10.1007/s00382-017-3830-7

Chen, D., & Dai, A. (2019). Precipitation characteristics in the community atmosphere model and their dependence on model physics and resolution. *Journal of Advances in Modeling Earth Systems*, *11*, 2352–2374. https://doi.org/10.1029/2018MS001536

Chen, J., Dai, A., Zhang, Y., & Rasmussen, K. L. (2020). Changes in convective available potential energy and convective inhibition under global warming. *Journal of Climate*, *33*(6), 2025–2050. https://doi.org/10.1175/JCLI-D-19-0461.1

Chikira, M., & Sugiyama, M. (2010). A cumulus parameterization with state-dependent entrainment Rate. Part I: Description and sensitivity to temperature and humidity profiles. *Journal of the Atmospheric Sciences*, *67*(7), 2171–2193. https://doi.org/10.1175/2010jas3316.1

Covey, C., Gleckler, P. J., Doutriaux, C., Williams, D. N., Dai, A., Fasullo, J., et al. (2016). Metrics for the diurnal cycle of precipitation: Toward routine benchmarks for climate models. *Journal of Climate*, *29*(12), 4461–4471. https://doi.org/10.1175/jcli-d-15-0664.1

Dai, A. (2006). Precipitation characteristics in eighteen coupled climate models. *Journal of Climate*, *19*, 4605–4630. https://doi.org/10.1175/JCLI3884.1

Dai, A., Lin, X., & Hsu, K. (2007). The frequency, intensity, and diurnal cycle of precipitation in surface and satellite observations over low- and mid-latitudes. *Climate Dynamics*, *29*, 727–744. https://doi.org/10.1007/s00382-007-0260-y

Dai, A., Rasmussen, R. M., Liu, C., Ikeda, K., & Prein, A. F. (2020). A new mechanism for warm-season precipitation response to global warming based on convection-permitting simulations. *Climate Dynamics*, *55*, 343–368. https://doi.org/10.1007/s00382-017-3787-6

Dai, A., & Trenberth, K. E. (2004). The diurnal cycle and its depiction in the community climate system model. *Journal of Climate*, *117*(2), 930–951. https://doi.org/10.1175/1520-0442(2004)017<0930:tdcaid>2.0.co;2

DeAngelis, A. M., Qu, X., Zelinka, M. D., & Hall, A. (2015). An observational radiative constraint on hydrologic cycle intensification. *Nature*, *528*(7581), 249–253. https://doi.org/10.1038/nature15770

Del Genio, A. D., Yao, M., Kovari, W., & Lo, K. K. (1996). A prognostic cloud water parameterization for global climate models. *Journal of Climate*, *9*, 270–304. https://doi.org/10.1175/1520-0442(1996)009<0270:APCWPF>2.0.CO;2

DeMott, C. A., Randall, D. A., & Khairoutdinov, M. (2007). Convective precipitation variability as a tool for general circulation model analysis. *Journal of Climate*, *20*, 91–112. https://doi.org/10.1175/JCLI3991.1

Donner, L. J., Coauthors, B. L., Hemler, R. S., Horowitz, L. W., Ming, Y., Zhao, M., et al. (2011). The dynamical core, physical parameterizations, and basic simulation characteristics of the atmospheric component AM3 of the GFDL global coupled model CM3. *Journal of Climate*, *24*, 3484–3519. https://doi.org/10.1175/2011JCLI3955.1

Emanuel, K. A. (1991). A scheme for representing cumulus convection in large-scale models. *Journal of the Atmospheric Sciences*, *48*, 2313–2329. https://doi.org/10.1175/1520-0469(1991)048<2313:ASFRCC>2.0.CO;2

Emori, S., Nozawa, T., Numaguti, A., & Uno, I. (2001). Importance of cumulus parameterization for precipitation simulation over East Asia in June. *Journal of the Meteorological Society of Japan*, *79*(4), 939–947. https://doi.org/10.2151/jmsj.79.939

Flato, G., Marotzke, J., Abiodun, B., Braconnot, P., Chou, S. C., Collins, W., et al. (2013). Evaluation of Climate Models. In T. F. Stocker, D. Qin, G.-K. Plattner, M. Tignor, S. K. Allen, J. Boschung, A. Nauels, Y. Xia, V. Bex, & P. M. Midgley (Eds.), *Climate change 2013: The physical science basis. Contribution of working group I to the fifth assessment report of the intergovernmental panel on climate change*. Cambridge: Cambridge University Press.

Gettelman, A., Morrison, H., & Ghan, S. J. (2008). A new two-moment bulk stratiform cloud microphysics scheme in the NCAR community atmosphere model (CAM3). Part II: Single-column and global results. *Journal of Climate*, *21*, 3660–3679. https://doi.org/10.1175/2008JCLI2116.1

Gregory, D. (2001). Estimation of entrainment rate in simple models of convective clouds. *Quarterly Journal of the Royal Meteorological Society*, *127*(53), 72. https://doi.org/10.1002/qj.49712757104

Gregory, D., & Rowntree, P. R. (1990). A mass flux convection scheme with representation of cloud ensemble characteristics and stability-dependent closure. *Monthly Weather Review*, *118*, 1483–1506. https://doi.org/10.1175/1520-0493(1990)118<1483:AMFCSW>2.0.CO;2

Held, I. M., Zhao, M., & Wyman, B. (2007). Dynamic radiative–convective equilibria using GCM column physics. *Journal of the Atmospheric Sciences*, *64*(1), 228–238. https://doi.org/10.1175/JAS3825.11

Hourdin, F., Musat, I., Bony, S., Braconnot, P., Codron, F., Dufresne, J. L., & Krinner, G. (2006). The LMDZ4 general circulation model: Climate performance and sensitivity to parametrized physics with emphasis on tropical convection. *Climate Dynamics*, *27*(7–8), 787–813. https://doi.org/10.1007/s00382-006-0158-0

Hourdin, F., Rio, C., Grandpeix, J. Y., Madeleine, J. B., Cheruy, F., Rochetin, N., & Foujols, M. A. (2020). LMDZ6A: The atmospheric component of the IPSL climate model with improved and better tuned physics. *Journal of Advances in Modeling Earth Systems*, *12*(7), e2019MS001892. https://doi.org/10.1029/2019ms001892

Houze, R. A., Rasmussen, K. L., Zuluaga, M. D., & Brodzik, S. R. (2015). The variable nature of convection in the tropics and subtropics: A legacy of 16 years of the tropical rainfall measuring mission satellite. *Review of Geophysics*, *53*, 994–1021. https://doi.org/10.1002/2015RG000488

Huffman, G. J., Adler, R. F., Bolvin, D. T., & Gu, G. (2009). Improving the global precipitation record: GPCP version 2.1. *Geophysical Research Letters*, *36*, L17808. https://doi.org/10.1029/2009GL040000

Huffman, G. J., Adler, R. F., Bolvin, D. T., Gu, G., Nelkin, E. J., Bowman, K. P., et al. (2007). The TRMM multisatellite precipitation analysis (TMPA): Quasi-global, multiyear, combined-sensor precipitation estimates at fine scales. *Journal of Hydrometeorology*, *8*, 38–55. https://doi.org/10.1175/JHM560.1

Kay, J. E., L'Ecuyer, T., Pendergrass, A., Chepfer, H., Guzman, R., & Yettella, V. (2018). Scale-aware and definition-aware evaluation of modeled near-surface precipitation frequency using CloudSat observations. *Journal of Geophysical Research: Atmospheres*, *123*, 4294–4309. https://doi.org/10.1002/2017JD028213

Kelley, M., Schmidt, G. A., Nazarenko, L. S., Bauer, S. E., Ruedy, R., Russell, G. L., & Canuto, V. (2020). GISS-E2. 1: Configurations and climatology. *Journal of Advances in Modeling Earth Systems*, *12*(8), e2019MS002025. https://doi.org/10.1029/2019ms002025

Kooperman, G. J., Pritchard, M. S., O'Brien, T. A., & Timmermans, B. W. (2018). Rainfall from resolved rather than parameterized processes better represents the present-day and climate change response of moderate rates in the community atmosphere model. *Journal of Advances in Modeling Earth Systems*, *10*(4), 971–988. https://doi.org/10.1002/2017MS001188

Kopparla, P., Fischer, E. M., Hannay, C., & Knutti, R. (2013). Improved simulation of extreme precipitation in a high-resolution atmosphere model. *Geophysical Research Letters*, *40*, 5803–5808. https://doi.org/10.1002/2013GL057866

Le Treut, H., & Li, Z. X. (1991). The sensitivity of an atmospheric general circulation model to prescribed SST changes: Feedback effects associated with the simulation of cloud optical properties. *Climate Dynamics*, *5*, 175–187.

Lin, Y., Zhao, M., Ming, Y., Golaz, J. C., Donner, L. J., Klein, S. A., & Xie, S. (2013). Precipitation partitioning, tropical clouds, and intraseasonal variability in GFDL AM2. *Journal of Climate*, *26*(15), 5453–5466. https://doi.org/10.1175/jcli-d-12-00442.1

Lohmann, U., & Roeckner, E. (1996). Design and performance of a new cloud microphysics scheme developed for the ECHAM general circulation model. *Climate Dynamics*, *12*, 557–572. https://doi.org/10.1007/s003820050128

Ma, Z., Liu, Q., Zhao, C., Shen, X., Wang, Y., Jiang, J. H., et al. (2018). Application and evaluation of an explicit prognostic cloud-cover scheme in GRAPES global forecast system. *Journal of Advances in Modeling Earth Systems*, *10*, 652–667. https://doi.org/10.1002/2017MS001234

Massonnet, F., Ménégoz, M., Acosta, M., Yepes-Arbós, X., Exarchou, E., & Doblas-Reyes, F. J. (2020). Replicability of the EC-Earth3 Earth system model under a change in computing environment. *Geoscientific Model Development*, *13*(3). https://doi.org/10.5194/gmd-13-1165-2020

Mizuta, R., Yoshimura, H., Murakami, H., Matsueda, M., Endo, H., Ose, T., et al. (2012). Climate simulations using MRI-AGCM3. 2 with 20-km grid. *Journal of the Meteorological Society of Japan. Ser. II*, *90*, 233–258. https://doi.org/10.2151/jmsj.2012-a12

Moorthi, S., & Suarez, M. J. (1992). Relaxed Arakawa–Schubert: A parameterization of moist convection for general circulation models. *Monthly Weather Review*, *120*, 978–1002. https://doi.org/10.1175/1520-0493(1992)120<0978:rasapo>2.0.co;2

Nordeng, T. E. (1994). Extended versions of the convective parameterization scheme at ECMWF and their impact on the mean and transient activity of the model in the tropics. *ECMWF Tech. Memo.*, *206*, 41.

O'Brien, T. A., Li, F., Collins, W. D., Rauscher, S. A., Ringler, T. D., Taylor, M. S., et al. (2013). Observed scaling in clouds and precipitation and scale incognizance in regional to global atmospheric models. *Journal of Climate*, *26*(23), 9313–9333. https://doi.org/10.1175/JCLI-D-13-00005.1

Pendergrass, A. G., & Hartmann, D. L. (2014). Changes in the distribution of rain frequency and intensity in response to global warming. *Journal of Climate*, *27*, 8372–8383. https://doi.org/10.1175/JCLI-D-14-00183.1

Prein, A. F., Rasmussen, R. M., Ikeda, K., Liu, C., Clark, M. P., & Holland, G. J. (2017). The future intensification of hourly precipitation extremes. *Nature Climate Change*, *7*(1), 48–52. https://doi.org/10.1038/nclimate3168

Qian, T., Dai, A., Trenberth, K. E., & Oleson, K. W. (2006). Simulation of global land surface conditions from 1948–2004. Part I: Forcing data and evaluation. *Journal of Hydrometeorology*, *7*, 953–975. https://doi.org/10.1175/JHM540.1

Rasch, P., & Kristjánsson, J. (1998). A comparison of the CCM3 model climate using diagnosed and predicted condensate parameterizations. *Journal of Climate*, *11*(7), 1587–1614. https://doi.org/10.1175/1520-0442(1998)011<1587:ACOTCM>2.0.CO;2

Rauscher, S. A., O'Brien, T. A., Piani, C., Coppola, E., Giorgi, F., Collins, W. D., & Lawston, P. M. (2016). A multimodel intercomparison of resolution effects on precipitation: Simulations and theory. *Climate Dynamics*, *47*, 2205–2218. https://doi.org/10.1007/s00382-015-2959-5

Ricard, J., & Royer, J. (1993). A statistical cloud scheme for use in an AGCM. *Annales Geophysicae*, *11*, 1095–1115.

Rosa, D., & Collins, W. D. (2013). A case study of subdaily simulated and observed continental convective precipitation: CMIP5 and multiscale global climate models comparison. *Geophysical Research Letters*, *40*(22), 5999–6003. https://doi.org/10.1002/2013GL057987

Sakaguchi, K., Leung, L. R., Burleyson, C. D., Xiao, H., & Wan, H. (2018). Role of troposphere-convection-land coupling in the southwestern Amazon precipitation bias of the community earth system model version 1 (CESM1). *Journal of Geophysical Research: Atmospheres*, *123*, 8374–8399. https://doi.org/10.1029/2018JD028999

Schmidt, G. A., Kelley, M., Nazarenko, L., Ruedy, R., Russell, G. L., Aleinov, I., et al. (2014). Configuration and assessment of the GISS ModelE2 contributions to the CMIP5 archive. *Journal of Advances in Modeling Earth Systems*, *6*, 141–184. https://doi.org/10.1002/2013MS000265

Schumacher, C., & Houze, R. A., Jr. (2003). Stratiform rain in the tropics as seen by the TRMM Precipitation Radar. *Journal of Climate*, *16*, 1739–1756. https://doi.org/10.1175/1520-0442(2003)016<1739:sritta>2.0.co;2

Smith, R. N. B. (1990). A scheme for predicting layer clouds and their water content in a general circulation model. *Quarterly Journal of the Royal Meteorological Society*, *116*, 435–460. https://doi.org/10.1002/qj.49711649210

Stephens, G. L., L'Ecuyer, T., Forbes, R., Gettelmen, A., Golaz, J. C., Bodas-Salcedo, A., et al. (2010). Dreary state of precipitation in global models. *Journal of Geophysical Research*, *115*(D24). https://doi.org/10.1029/2010JD014532

Tatebe, H., Ogura, T., Nitta, T., Komuro, Y., Ogochi, K., Takemura, T., et al. (2019). Description and basic evaluation of simulated mean state, internal variability, and climate sensitivity in MIROC6. *Geoscientific Model Development*, *12*(7), 2727–2765. https://doi.org/10.5194/gmd-12-2727-2019

Thackeray, C. W., Qu, X., & Hall, A. (2018). Why do models produce spread in snow albedo feedback? *Geophysical Research Letters*, *45*(12), 6223–6231. https://doi.org/10.1029/2018gl078493

Tiedtke, M. (1989). A comprehensive mass flux scheme for cumulus parameterization in large-scale models. *Monthly Weather Review*, *117*, 1779–1800. https://doi.org/10.1175/1520-0493(1989)117<1779:ACMFSF>2.0.CO;2

Tiedtke, M. (1993). Representation of clouds in large-scale models. *Monthly Weather Review*, *121*(2), 3040–3061. https://doi.org/10.1175/1520-0493(1993)121<3040:rocils>2.0.co;2

Trenberth, K. E. (2011). Changes in precipitation with climate change. *Climate Research*, *47*, 123–138. https://doi.org/10.3354/cr00953

Trenberth, K. E., Dai, A., Rasmussen, R. M., & Parsons, D. B. (2003). The changing character of precipitation. *Bulletin of the American Meteorological Society*, *84*, 1205–1218. https://doi.org/10.1175/BAMS-84-9-1205

Trenberth, K. E., & Zhang, Y. (2018). How often does it really rain? *Bulletin of the American Meteorological Society*, *99*, 289–298. https://doi.org/10.1175/BAMS-D-17-0107.1

Tropical Rainfall Measuring Mission (TRMM). (2011a). *TRMM (TMPA) Rainfall Estimate L33 hour 0.25 degree x 0.25 degree V7, Greenbelt, MD, Goddard Earth Sciences Data and Information Services Center (GES DISC)*. https://doi.org/10.5067/TRMM/TMPA/3H/7

Tropical Rainfall Measuring Mission (TRMM). (2011b). *TRMM radar rainfall statistics L3 1month (5 x 5) and (0.5 x 0.5) degree V7, Greenbelt, MD, Goddard Earth Sciences data and information services center*. Retrieved from https://disc.gsfc.nasa.gov/datacollection/TRMM_3A25_7.html

Voldoire, A., Saint-Martin, D., Sénési, S., Decharme, B., Alias, A., Chevallier, M., et al. (2019). Evaluation of CMIP6 DECK experiments with CNRM-CM6-1. *Journal of Advances in Modeling Earth Systems*, *11*, 2177–2213. https://doi.org/10.1029/2019MS001683

Watanabe, M., Suzuki, T., O'ishi, R., Komuro, Y., Watanabe, S., Emori, S., et al. (2010). Improved climate simulation by MIROC5: Mean states, variability, and climate sensitivity. *Journal of Climate*, *23*(23), 6312–6335. https://doi.org/10.1175/2010jcli3679.1

Watanabe, S., Hajima, T., Sudo, K., Nagashima, T., Takemura, T., Okajima, H., et al. (2011). MIROC-ESM 2010: Model description and basic results of CMIP5-20c3m experiments. *Geoscientific Model Development*, *4*, 845–872. https://doi.org/10.5194/gmd-4-845-2011

Wehner, M. F., Reed, K. A., Li, F., Prabhat, Bacmeister, J., Chen, C.-T., et al. (2014). The effect of horizontal resolution on simulation quality in the community atmosphere model, CAM5.1. *Journal of Advances in Modeling Earth Systems*, *6*, 980–997. https://doi.org/10.1002/2013MS000276

Westra, S., Fowler, H. J., Evans, J. P., Alexander, L. V., Berg, P., Johnson, F., et al. (2014). Future changes to the intensity and frequency of short-duration extreme rainfall. *Reviews of Geophysics*, *52*(3), 522–555. https://doi.org/10.1002/2014rg000464

Wilcox, E. M., & Donner, L. J. (2007). The frequency of extreme rain events in satellite rain-rate estimates and an atmospheric general circulation model. *Journal of Climate*, *20*(1), 53–69. https://doi.org/10.1175/JCLI3987.1

Williamson, D. L. (2013). The effect of time steps and time-scales on parametrization suites. *Quarterly Journal of the Royal Meteorological Society*, *139*, 548–560. https://doi.org/10.1002/qj.1992

Wilson, D. R., & Ballard, S. P. (1999). A microphysically based precipitation scheme for the UK meteorological office unified model. *Quarterly Journal of the Royal Meteorological Society*, *125*, 1607–1636. https://doi.org/10.1002/qj.49712555707

Wu, T. (2012). A mass-flux cumulus parameterization scheme for large-scale models: Description and test with observations. *Climate Dynamics*, *38*, 725–744. https://doi.org/10.1007/s00382-011-0995-3

Xie, S. C., Zhang, M. H., Boyle, J. S., Cederwall, R. T., Potter, G. L., & Lin, W. Y. (2004). Impact of a revised convective triggering mechanism on community atmosphere model, version 2, simulations: Results from short-range weather forecasts. *Journal of Geophysical Research*, *109*, D14102. https://doi.org/10.1029/2004JD004692

Yang, S., & Smith, E. A. (2008). Convective–stratiform precipitation variability at seasonal scale from 8 yr of TRMM observations: Implications for multiple modes of diurnal variability. *Journal of Climate*, *21*(16), 4087–4114. https://doi.org/10.1175/2008JCLI2096.1

Yao, M. S., & Del Genio, A. D. (1989). Effects of cumulus entrainment and multiple cloud types on a January global climate model simulation. *Journal of Climate*, *2*, 850–863. https://doi.org/10.1175/1520-0442(1989)002<0850:eoceam>2.0.co;2

Yukimoto, S., Adachi, Y., Hosaka, M., Sakami, T., Yoshimura, H., Hirabara, M., et al. (2012). A new global climate model of the Meteorological Research Institute: MRI-CGCM3—Model description and basic performance. *Journal of the Meteorological Society of Japan. Ser. II*, *90*, 23–64. https://doi.org/10.2151/jmsj.2012-a02

Zhang, G. J. (2002). Convective quasi-equilibrium in midlatitude continental environment and its effect on convective parameterization. *Journal of Geophysical Research*, *107*(D14). https://doi.org/10.1029/2001jd001005

Zhang, G. J., & McFarlane, N. A. (1995). Sensitivity of climate simulations to the parameterization of cumulus convection in the Canadian climate centre general circulation model. *Atmosphere-Ocean*, *33*(3), 407–446. https://doi.org/10.1080/07055900.1995.9649539

Zhang, G. J., & Mu, M. (2005). Effects of modifications to the Zhang-McFarlane convection parameterization on the simulation of the tropical precipitation in the national center for atmospheric research community Climate Model, version 3. *Journal of Geophysical Research*, *110*, D09109. https://doi.org/10.1029/2004JD005617

Zhang, M., Lin, W., Bretherton, C. B., Hack, J. J., & Rasch, P. J. (2003). A modified formulation of fractional stratiform condensation rate in the NCAR community atmosphere model (CAM2). *Journal of Geophysical Research*, *108*, 4035. https://doi.org/10.1029/2002JD002523

Zhao, M., Golaz, J.-C., Held, I. M., Guo, H., Balaji, V., Benson, R., et al. (2018). The GFDL global atmosphere and land model AM4.0/LM4.0: 2. Model description, sensitivity studies, and tuning strategies. *Journal of Advances in Modeling Earth Systems*, *10*, 735–769. https://doi.org/10.1002/2017MS001209

Zhou, T. J., Yu, R. C., Chen, H. M., Dai, A., & Pan, Y. (2008). Summer precipitation frequency, intensity, and diurnal cycle over China: A comparison of satellite data with rain gauge observations. *Journal of Climate*, *21*, 3997–4010. https://doi.org/10.1175/2008JCLI2028.1